Uncertainty estimates for 1-h averaged turbulence fluxes of carbon dioxide, latent heat and sensible heat

By DEAN VICKERS[1]*, MATHIAS GÖCKEDE[2] and BEVERLY E. LAW[2],   [1]*College of Oceanic and Atmospheric Sciences, Oregon State University, COAS Admin Bldg 104, Corvallis, OR 97331, USA;* [2]*College of Forestry, Oregon State University, Corvallis, OR 97331-5704, USA*

ABSTRACT

A new observational approach is presented to approximate the uncertainty (scatter or error variance) in 1-h averaged turbulence fluxes from eddy-covariance measurements. The uncertainty includes potential contributions from instrument problems, heterogeneity and non-stationarity in addition to classical random sampling error. The daytime relative flux uncertainty (RFE) is half as large (20%) at a simple maize site compared to two more complex forest sites (40%) for all scalars possibly due to the more homogeneous vegetation, flat terrain and especially the lower measurement height. The RFE is approximately the same for day and night periods for all scalars at the two mostly homogeneous sites (pine forest and maize field) except for latent heat over the forest, where the RFE doubles at night. Modest surface heterogeneity at the other forest site for nocturnal flux footprints approximately doubles the RFE compared to daytime conditions for all scalar fluxes. Compositing by atmospheric stability (instead of time of day) reveals a sharp increase in the RFE for the most strongly stable conditions. A theoretical prediction for the pure random sampling error based on the flux integral timescale is smaller by a factor of two compared to the observed variability.

1. Introduction

Eddy-covariance flux measurements are now being collected at over 400 sites globally (van Gorsel et al., 2007). In addition to documenting the means of the observed fluxes on short timescales for different ecosystems and climates, reliable estimates for the flux uncertainties are needed to improve model validation and data assimilation in process-based carbon models (e.g. Thorton et al., 2002; Williams et al., 2005), inverse modeling studies (e.g. Lasslop et al., 2008) and model-data synthesis (Braswell et al., 2005; Knorr and Kattge, 2005), where the uncertainties may be as important as the fluxes themselves (Raupach et al., 2005). There is interest in short-term (1-h averaged) fluxes as process models strive to predict short-term changes in scalar fluxes, for example, understanding how the carbon dioxide flux changes from early morning to late morning in response to increasing radiation, temperature and vapour pressure deficit. Error bars on the observed fluxes are required to assess model performance. Uncertainty (scatter or error variance) in the short-term average eddy-covariance flux may originate from: (1) instrument problems (e.g. attack angle-dependent flow distortion and instrument separation Foken et al., 2004),

(2) a variable flux footprint in a heterogeneous landscape causing the fluxes to be unrepresentative of the targeted ecosystem for a subset of meteorological conditions (e.g. Schmid, 2002; Göckede et al., 2008), (3) non-stationarity (e.g. diurnal trend) and (4) classical random error due to inadequate sampling of the turbulence (Lenschow et al., 1994).

The theoretical development of Lenschow et al. (1994) and Mann and Lenschow (1994) showed that the contribution to the relative flux uncertainty from pure random sampling error (item 4 above) is proportional to the square root of the ratio of the integral length scale (a characteristic of the turbulence) divided by the flux averaging length scale (scale over which the products of perturbations are averaged). Their results applied to tower measurements indicate that a four-fold increase in the flux averaging timescale is required to reduce the relative random error by a factor of two, and that in practice it is much more difficult to reduce the random error to acceptable levels than to reduce the systematic error, where the systematic error here refers to a failure to capture all the transporting scales often leading to an underestimate of the flux. Due to other sources of uncertainty (listed above), the classical approach for the random sampling error is expected to be less than the total observed uncertainty.

Different observational approaches have been proposed for estimating flux uncertainty (Mahrt, 1998; Howell and Sun, 1999; Hollinger and Richardson, 2005; Richardson et al., 2006;

Lasslop et al., 2008; Richardson et al., 2008; Vickers et al., 2009). Observational approaches typically estimate the uncertainty by making multiple measurements of the flux under similar environmental conditions and then use the variability of such measurements to estimate a standard deviation that represents uncertainty (e.g. Hollinger and Richardson, 2005). Richardson et al. (2008) examined the difference between a model-based prediction of the flux and the observed 30-min average flux to estimate the flux uncertainty. Hollinger and Richardson (2005) used two approaches: (1) the difference between coincident 30-min average fluxes measured on two nearby towers (two-tower method) and (2) the difference between observed fluxes made on the same tower at the same local time on two successive days with similar environmental conditions (daily-differencing approach). The two-tower approach is not feasible for most flux sites and may introduce spatial variability into the problem. As noted by Hollinger and Richardson (2005), limitations of the daily-differencing approach include changes in environmental conditions during the intervening 24-h period (e.g. rain, frost, etc.), and changes in conditions that are undetected by tower measurements (e.g. advection, boundary-layer depth). In addition, the requirement of similar environmental conditions 24-h apart reduces the data sample size available for calculating the uncertainty. Lasslop et al. (2008) defined random flux error as the difference between the measured flux and the expected value of the flux using measurements under similar meteorological conditions in a 14-d time window, and found uncertainty estimates comparable to the daily-differencing method. This last approach suffers from the same limitations as the daily-differencing method.

Hollinger and Richardson (2005) found that the frequency distribution of the 30-min average flux differences (two-tower method) was closer to double exponential than Gaussian in shape, and that the flux uncertainty increased linearly with the magnitude of the flux. They suggested that the increase in uncertainty with increasing flux magnitude may be related to inadequate sampling of the large eddies in daytime convective conditions, when the largest flux magnitudes are observed. They reported larger uncertainty estimates based on the daily-differencing approach compared to the two-tower method. Dragoni et al. (2007) found that the daily-differencing method overestimated the flux uncertainty by a factor of two at their site, and proposed that using two sensors at the same height on the same tower is the preferred method to estimate random measurement error.

In this work, we present a new observational approach that estimates the uncertainty in the record-averaged (1-h averaged) turbulence flux by examining the flux variability on subrecord scales (5-min). This is based on the fact that for stationary conditions, the random variability within a record predicts the variability between records (Bendat and Piersol, 1986; Mahrt, 1998). Our uncertainty estimates are for the vertical turbulence 1-h averaged flux, and do not include uncertainty related to other terms

in the budget equations (e.g. storage and advection). The new approach coupled with previous work may be useful for strengthening data quality and quantifying uncertainty in turbulence flux measurements used in data assimilation or model comparison studies. The observational estimates of the total flux uncertainty are contrasted with theoretical estimates for the classical random sampling error. We do not address potential systematic errors related to the instrumentation. The measurements are collected over a tall homogeneous ponderosa pine forest located on a saddle surrounded by complex terrain, and a short ponderosa pine plantation surrounded by a heterogeneous landscape of older taller pines and clearings in relatively flat terrain. Two years of data are used for analysis at the pine forest sites. A smaller data set from a homogeneous maize field is used to contrast with the forest sites. Measurements from a grassland site are used to examine the measurement height dependence (profile) of the flux uncertainty.

2. Data

2.1. Mature pine forest

The first data set analyzed is from a 90-yr-old mature ponderosa pine forest in central Oregon, USA (44.451°N latitude, 121.558°W longitude, 1255 m elevation) with continuous measurements during 2004 and 2005 (Schwarz et al., 2004; Thomas et al., 2009). The canopy extends from approximately 10 to 16 m above ground, while the understory consists of scattered 1-m tall shrubs (bitterbrush and manzanita). The canopy is open such that the forest floor and understory receive direct sunlight during the day and are mostly open to the sky at night, leading to a large diurnal cycle of the subcanopy stability (Lee and Mahrt, 2005). The leaf area index (LAI) ranges from 3.1 to 3.4 during the growing season. The stand density is 325 trees ha^{-1} and the soil is sandy loam. Although the site is located on a relatively flat saddle region about 600 m across, it is surrounded by complex terrain. Imagery and surveys indicate that this age class of ponderosa pine is prevalent for several kilometres in all directions except to the north where there is a logged area beginning approximately 500 m from the tower. The dominate flow direction is from the southwest throughout the year. Eddy-covariance flux measurements were collected using a Campbell Scientific CSAT3 sonic anemometer and open-path LICOR-7500 gas analyser deployed at 31 m above ground (or about twice the canopy height).

2.2. Young pine forest

The second data set is from a 3-m tall, young ponderosa pine plantation with seasonal grass understory in central Oregon, USA (44.315 N latitude, 121.608 W longitude, 1005 m elevation) during 2004 and 2005. The site was clear cut and replanted by the U.S. Forest Service in 1987. The stand density

is 260 trees ha^{-1} and the peak LAI was 0.61 and 0.71 in 2004 and 2005, respectively. The dimensions of the area with the uniform young pines is 300×375 m, and the flux tower is located approximately in the centre. The terrain slopes upward at about 2% to the west and southwest, and slopes weakly downward (<1%) or is flat in other directions. Eddy-covariance measurements were collected using a Campbell Scientific CSAT3 sonic anemometer and open-path LICOR-7500 gas analyser deployed at 12 m above ground (or about four times the canopy height).

A heterogeneous stand of older (20–100 yr) and taller (5–30 m) ponderosa pines surround the site on three sides. The area located 300–600 m upwind from the tower for the most frequently observed wind directions between 220 and 300° is characterized by irregular patches of short vegetation and/or clearings embedded within the older stand. The scale of individual patches is on the order of a hundred metres. A larger clearing is located 1 km upwind for winds from 200° to 220°. An anomalously wet region (Cold Springs) is located approximately 2 km upwind from the tower for flow from 245°. Compared to the mature pine site, the young site is more heterogeneous in terms of vegetation type when the flux footprint is outside the plantation, more homogeneous when the footprint is inside the plantation and more homogeneous in terms of terrain height.

2.3. Maize fields

Eddy-covariance flux data were were collected over two maize fields near Ames, Iowa, USA for a 1-month period beginning in early June (emergence) and running until full canopy in July of 2005 as part of the Soil Moisture Experiment (SMEX05) (Yilmaz et al., 2008; Cosh et al., 2009). Both measurement sites are in flat terrain with large homogeneous fetch. Campbell CSAT3 sonic anemometers and open-path LICOR-7500 gas analyzers were deployed at 4 m above ground. The height of the maize canopy grew from 0.5 to 2 m during the experiment. Due to the short data record and the strong similarity between the two sites, we pool the data from the two flux towers into a single maize data set.

2.4. CASES

A grassland data set from the Cooperative Atmosphere-Surface Exchange Study (CASES) in Kansas, USA, during October of 1999 (Poulos et al., 2002) is used to examine the height dependence of the flux uncertainty for sensible heat. CO_2 and latent heat fluxes are not available from this data set. CASES was designed to study the structure of the stable boundary layer. The measurements were collected by the Atmospheric Technology Division of the National Center for Atmospheric Research (NCAR). We include sonic anemometer data from the 10, 20, 30, 40 and 50-m levels on the NCAR main 60-m tower and from the 1 and 5-m levels on the UConn mini-tower located 10 m from the main tower.

3. Methods

3.1. Quality control

It is crucial to identify and remove all suspect data associated with instrument failures (e.g. moisture on the sensors) prior to estimating the flux uncertainty. The quality control testing we apply to the fast response time series is designed to detect instrument problems, and does not eliminate any data based on criterion associated with wind speed, mixing strength, flux footprint or agreement with similarity theory. Our intention is to examine all data that survive the tests for instrument problems, whether or not the data satisfy similarity theory or well-developed turbulence criteria. In complex terrain, over a heterogeneous landscape or in the roughness sublayer, one would not expect similarity theory to always hold. The revised software package (the original package was described in Vickers and Mahrt, 1997) applies tests to the set of fast response variables to detect: (1) too many spikes (spikes are subsequently removed using an iterative procedure prior to further testing), (2) a value outside a defined valid range, (3) unusually large skewness or kurtosis, (4) large discontinuities detected using the Haar transform and (5) a variance that is outside a defined valid range (a variance that is either too small or too large is flagged). The Haar transform calculates the difference in some quantity over two half window means. Large values of the transform identify changes which are coherent on the scale of the window. The quality control tests are applied to over-lapping windows of width 10 min that move sequentially through the records. Variables that are flagged by any of the tests are plotted for visual inspection and either confirmed as an instrument problem (and subsequently removed from further analysis) or identified as unusual but plausible data and retained for further analysis.

It is our experience that it is much more difficult to identify all the suspect data from the open-path LICOR compared to the sonic anemometer. Therefore, in addition to the standard quality control testing, we also discard records where the CO_2 or latent heat flux event flag (Vickers and Mahrt, 1997) exceeds 20, indicating that the maximum 5-minute flux within the 1-hour record is 20 times larger than the record-mean flux. These rare events occur under two situations: (1) when the record-mean flux approaches zero as it changes sign during the morning or evening transition period and (2) when a record with subtle (or short lived) instrument problems manages to pass the automated quality control testing without raising a flag. The instrument problems were verified by plotting the raw time series. The same quality control procedures were applied to the raw fast response variables for all four data sets.

3.2. Coordinate rotation

A tilt correction (or coordinate rotation) based on the average wind direction dependence of the tilt angle is applied to the

fast-response wind components (Paw et al., 2000; Feigenwinter et al., 2004). The tilt correction does not force the mean vertical motion to zero for individual records. The planar-fit approach (Wilczak et al., 2001) is an idealized case of the approach used here. For perfectly planar topography and a perfectly leveled anemometer, or, for perfectly flat terrain and a vertically tilted anemometer, the tilt correction method used here reduces to the planar fit method. The same software was applied to all four data sets.

3.3. Flux calculations

We choose 1-hr data records as a compromise. Shorter records have the advantage of weaker non-stationarity, however, longer records are required to obtain enough independent samples of the subrecord flux with minimal systematic flux error. Systematic error here refers to a failure to capture all of the turbulence scales, often leading to an underestimate of the flux.

We choose a constant 5-min perturbation timescale to calculate the fluxes as a compromise between unstable and stable conditions. Turbulence in stable conditions is typically confined to timescales of a few minutes or less, while motions on timescales longer than a few minutes do not generally have characteristics of turbulence (e.g. the motions are primarily horizontal not three-dimensional), and the associated fluxes have very large scatter and are often unrelated to the local sources and sinks (Acevedo et al., 2006, 2007; Mahrt and Vickers, 2006; Vickers and Mahrt, 2006a; van den Kroonenberg and Bange, 2007). It is useful to exclude these longer timescale motions from this analysis because the flux uncertainty at turbulence scales and the flux uncertainty associated with non-turbulent scales may have very different sources (Mahrt, 2009). Note that transport on scales longer than the perturbation timescale is not included in the calculated turbulence flux, and must appear as advection in the budget equations.

In addition, little confidence can be placed in the small values of the measured vertical velocity at longer (30-min) timescales. Independent estimates of vertical velocity from the horizontal divergence exhibited more stable estimates of the average vertical motion compared to the direct estimate from the sonic anemometer (Vickers and Mahrt, 2006b). Also, the vertical velocity at longer timescales is more sensitive to the details of the tilt rotation compared to the turbulence vertical velocity.

Use of a shorter perturbation timescale would increase the systematic flux error in unstable conditions. Previous work at the pine forest sites indicates that the systematic flux error is about 10% when using a 5-min perturbation timescale in the worst-case convective conditions (Vickers et al., 2009). The systematic error is much smaller in near-neutral and stable conditions. The 10% systematic error in the convective subrecord fluxes is not a major concern here because our focus is more on the variability of the flux than the precise magnitude of the flux.

Use of a variable perturbation timescale depending on the characteristics of the turbulence for individual records (Vickers and Mahrt, 2006a) could be used, however, the additional complication may not be justified here. One such complication would be that the number of independent samples of the flux would vary for each record and vary systematically with atmospheric stability.

3.4. Flux uncertainty

Our approach is implemented by dividing each 1-h record into 12 non-overlapping subrecords of width $L = 5$ minutes. L defines the width of the subrecords, the perturbation timescale and the flux averaging timescale. The average subrecord fluxes (F_i) are calculated, where subscript i denotes the ith subrecord ($i = 1, N$), where $N = 12$ is the number of subrecords in a single 1-h record. The subrecord fluxes are partitioned into a record-mean value ($\langle F \rangle$), a linear trend component (F_i^T) and a random part (F_i^*), such that

$$F_i = \langle F \rangle + F_i^T + F_i^*. \tag{1}$$

To assess the flux uncertainty we compute

$$FE \equiv \sigma_{F^*}, \tag{2}$$

where σ_{F^*} is the observed standard deviation of the random part of the flux (F_i^*). This quantity is a measure of uncertainty of the record-average of the subrecord fluxes, and as such is a measure of the uncertainty in the 1-hour average flux. We express the flux uncertainty (FE) in terms of the standard deviation to be consistent with Hollinger and Richardson (2005).

The contribution to flux variability associated with linear trend (σ_{F^T}) is removed to help satisfy the stationarity condition. We note that even after removing the time trend in the subrecord fluxes, the turbulence may still be non-stationary and may be non-equilibrium. The trend in the fluxes across the record is approximated using linear regression of the subrecord fluxes on time. It turns out that σ_{F^T} is small compared to σ_{F^*} for the sites studied here except during the morning and evening transition periods just after sunrise and just before sunset, when the net radiation changes sign and σ_{F^T} can be of comparable magnitude to σ_{F^*}. Therefore, our uncertainty estimates (FE) are not especially sensitive to including the F_i^T term in eq. (1) except during transition periods.

The non-dimensional relative flux uncertainty is given by

$$RFE \equiv \frac{FE}{|\langle F \rangle|}. \tag{3}$$

The relative uncertainty is desirable for between-site comparisons because it accounts for the dependence of the flux uncertainty on the magnitude of the flux, which is different at every site. Non-dimensional quantities are more likely to be universal. The relative flux uncertainty is not well posed when the record-mean flux approaches zero, however, this problem is mitigated

by first averaging the numerator and the denominator and then taking the ratio when compositing by time of day or stability.

3.5. Theoretical random sampling error

The observational estimates of relative flux uncertainty are compared to a theoretical expression for the relative random sampling error,

$$\text{RSE} \equiv \frac{\sigma_F}{\langle F \rangle} = \left(\frac{2\tau}{T}\right)^{0.5} \left(\frac{1+r^2}{r^2}\right)^{0.5}, \tag{4}$$

where τ is the flux integral timescale, T is the averaging time (1 hr) and r is the correlation coefficient between the vertical velocity and the scalar considered (Lenschow et al., 1994; Mann and Lenschow, 1994; Finkelstein and Sims, 2001). The estimate of RSE is strongly sensitive to errors in the flux integral scale and the correlation for very small values of both (Fig. 1). The concept of an integral timescale, and therefore the above expression for the random sampling error, requires truly stationary time series.

For the purpose of evaluating eq. (4), we estimate the flux integral timescale by fitting an exponential to the observed autocorrelation function of the flux (Kaimal and Finnigan, 1994). This method may introduce errors when the autocorrelation function is not well represented by an exponential. As a sensitivity test, we averaged the autocorrelation functions over all records (separately by time of day for the growing season) and then fit the average autocorrelation function to an exponential. This method gave similar estimates for the flux integral timescale as the method where the timescale is computed for each record individually and then averaged. We elected not to integrate the area under the autocorrelation function to estimate the integral timescale (Finkelstein and Sims, 2001) because the function often approaches a non-zero constant value at large lag, in which

case the integral does not converge and the estimate of the integral timescale becomes dependent on the largest lag included in the integration.

Typical values for the flux integral timescale over the pine forests are 2–4 s during the day and and 1–2 s at night, with little variation between scalars. The longer timescale found for daytime periods is consistent with larger turbulent eddies associated with convection. The typical flux integral timescale over the maize (at the low measurement height of 4 m) is about 0.5 s with little variation between day and night and between scalars, consistent with smaller mean eddy size close to the ground. The small variation between day and night at the maize site is consistent with the reduced influence of stability closer to the ground. The flux integral timescale is considerably smaller than the timescale associated with the peak of the vertical velocity spectra, which ranges from 5 to 15 s over the forests and 2–4 s over the maize, depending on stability. The correlation coefficient between the vertical velocity and the scalar is typically 0.25–0.5 during the day and 0.05–0.3 at night. The highest correlations with vertical velocity for day and night tend to be for temperature (sensible heat flux).

4. Results

The dimensional flux uncertainty (FE, eq. 2) is greater during the stronger growth season compared to the rest of the year (Fig. 2), and is greater during the day compared to at night during the strong growth season (Fig. 3). The patterns in Figs. 2 and 3 indicate that the FE scales with the magnitude of the flux (Fig. 4), as reported by Hollinger and Richardson (2005) using the two-tower and daily-differencing approaches for estimating the uncertainty (Introduction). The large nocturnal FE for the CO_2 flux at the young site is discussed below. Unlike Richardson et al. (2006), we find a strong seasonal pattern in the sensible heat flux uncertainty (Fig. 2) that corresponds to the seasonal pattern of the sensible heat flux magnitude. Note that the turbulence CO_2 fluxes in Fig. 4 may not represent the net ecosystem exchange of CO_2 because of the potential importance of other terms in the carbon budget, namely, the storage and advection terms (Finnigan et al., 2003; Finnigan, 2004; Leuning et al., 2008).

We find a linear or less than linear dependence of the FE on flux magnitude, although the details of the relationships vary by site and by scalar flux (Fig. 5). For comparison to previous work, Fig. 5 includes linear fits from Richardson et al. (2006) using the daily-differencing method for a composite eastern U.S. forest and a grassland site. We find larger slopes (faster increase in FE with flux magnitude) at the mature pine site for daytime fluxes compared to Richardson et al. (2006) for their composite forest, and increases in FE that are less than linear for the nocturnal CO_2 flux and the daytime sensible heat flux at the maize site. Given that the flux uncertainty FE may include contributions from a number of sources, and therefore is probably site-specific, we cannot place too much significance on all of the differences
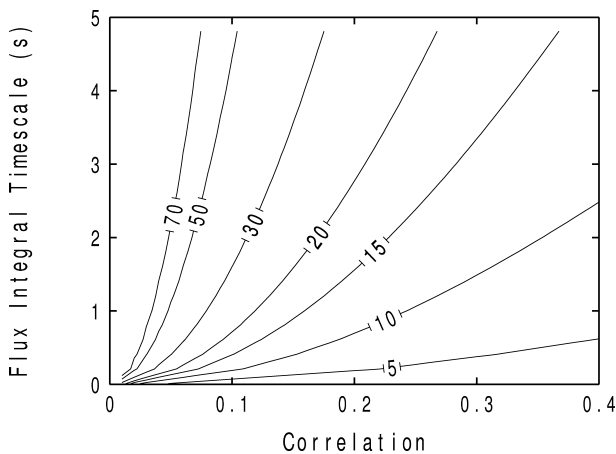

Fig. 1. Theoretical prediction of the classical random sampling error (RSE, eq. 4, percent) as a function of the flux integral timescale and the correlation.
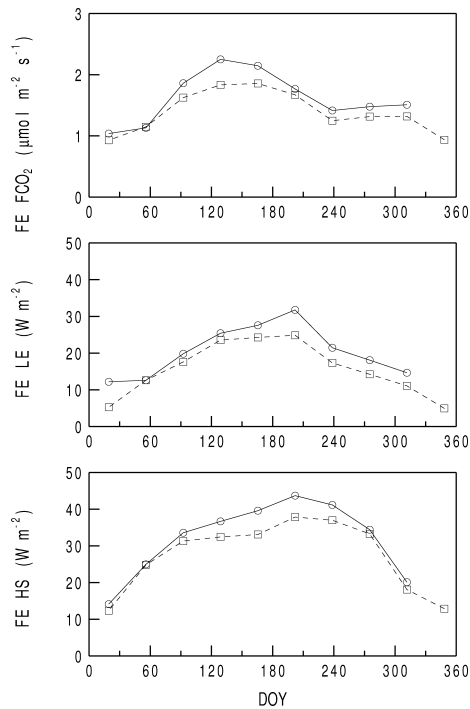
Fig. 2. Seasonal pattern of the flux uncertainty (FE) for the CO_2 flux (FCO_2) and the latent (LE) and sensible (HS) heat fluxes for the mature pine (circles, solid) and young pine (squares, dash) forests for all the 2004–2005 data combined. Each of the bins contains approximately 10% of the available data.

in Fig. 5, however, both our results and those of Richardson et al. (2006) strongly suggest that the relative flux uncertainty is greater at forest sites compared to either grassland or crop (maize) sites.

4.1. Time of day composites

To examine the differences between scalars and between sites in more detail we now focus on the time of day dependence of the relative (or normalized) flux uncertainty (RFE, eq. 3) (Fig. 6, Table 1). For reference, the corresponding dimensional flux uncertainties are listed in Table 2. The daytime RFE estimates vary by site more than by scalar, and are smaller at the maize site by about a factor of two (Fig. 6). Averaging over the three scalar fluxes, the mean daytime relative uncertainty in the 1-h averaged turbulence flux is 43, 37 and 18% at the mature pine, young pine and maize sites, respectively (Table 1).

There is evidence of enhanced relative uncertainty during the morning and evening transition periods for CO_2 and sensible heat fluxes, but not for latent heat (Fig. 6). Vickers and Mahrt (1997) found that the flux is in general more erratic with large non-stationarity. Recall that the direct influence of non-stationarity due to trends on timescales of one hour or more is removed (albeit imperfectly) from the estimates of FE and RFE by removing any
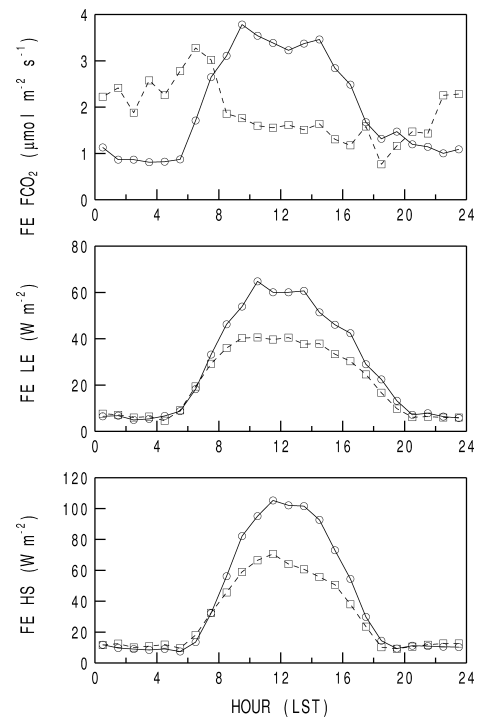

Fig. 3. Diurnal pattern of the flux uncertainty (FE) during the strong growth season (May–June–July of 2004–2005 combined) for the mature pine (circles, solid) and young pine (squares, dash) forests.

linear trend in the subrecord fluxes. The uncertainty in the latent heat flux is not enhanced during the transition periods, as it is for the CO_2 and sensible heat fluxes, probably because the mean specific humidity has a weaker time of day dependence.

Smaller relative uncertainty at the maize site may be related to the more homogeneous vegetation, flat topography and lower measurement height compared to the forests. Previous studies suggest that contributions to the vertical velocity variance from the larger eddies may be suppressed near the ground due to distortion by the mean wind shear and the blocking action of the surface (Caugheyand and Readings, 1975; Deardorff and Willis, 1985; Hunt and Carlotti, 2001). Because the larger eddies are the most poorly sampled, a reduction in their influence near the ground might reduce the flux uncertainty for lower measurement heights. These same arguments are consistent with finding the largest daytime RFE estimates at the mature pine site, which has the highest measurement height.

The CASES data support a measurement height dependence of the flux uncertainty in unstable conditions (Fig. 7), at least for the sensible heat flux (CO_2 and latent heat fluxes were not available from CASES). For this Kansas grassland site, the daytime flux uncertainty increases strongly with measurement height up to a height of approximately 20 m, and then remains relatively constant for heights from 20 m to the top of the tower. If we apply the observed measurement height dependence of RFE for sensible heat to the maize site by scaling the daytime RFE at
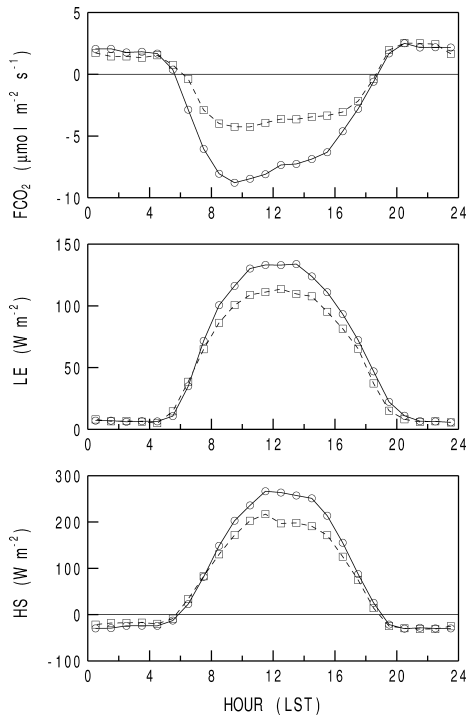
Fig. 4. Diurnal pattern of the flux during the strong growth season (May–June–July of 2004–2005 combined) for the mature pine (circles, solid) and young pine (squares, dash) forests.

Fig. 5. The flux uncertainty (FE) as a function of the flux magnitude during the strong growth season (May–June–July of 2004–2005 combined) for the mature pine (circles, solid) and young pine (squares, dash) forests, and for the maize data set (box-cross, dots) in June–July of 2005. The heavy solid lines are a forest composite and the heavy dashed lines are a grassland site from table 4 in Richardson et al. (2006).

4 m up to a height of 20 m using the CASES profile, the daytime RFE estimate at 20 m over the maize becomes about 35%, which is only slightly smaller than the estimates over the two forests. While inconclusive without more detailed measurements, this suggests that measurement height may explain most of the difference in the daytime RFE between the forest sites and the maize site.

Unlike the sensible heat flux, the latent heat flux relative uncertainty nearly doubles at night at the mature pine site. Although we have no direct evidence for these data sets, this may be related to the more complex sources of moisture compared to temperature. Andreas et al. (1998) found that sources and sinks of moisture are more heterogeneous than those for heat on fine-scales (metres), and that the impact of fine-scale heterogeneity on the flux variability is enhanced at night by a reduction of horizontal mixing in stable conditions. During the day, when the significance of fine-scale heterogeneity is reduced by stronger horizontal mixing, the flux uncertainty is approximately the same for all three scalar fluxes. The large relative uncertainty for latent heat at night (84%) corresponds to only 6 W m^{-2} (Tables 1 and 2) because the latent heat flux is small at night.

At the young pine forest the relative uncertainty is considerably larger at night compared to the day for all three scalars. Our interpretation is that the nocturnal RFE estimates for the young pine site i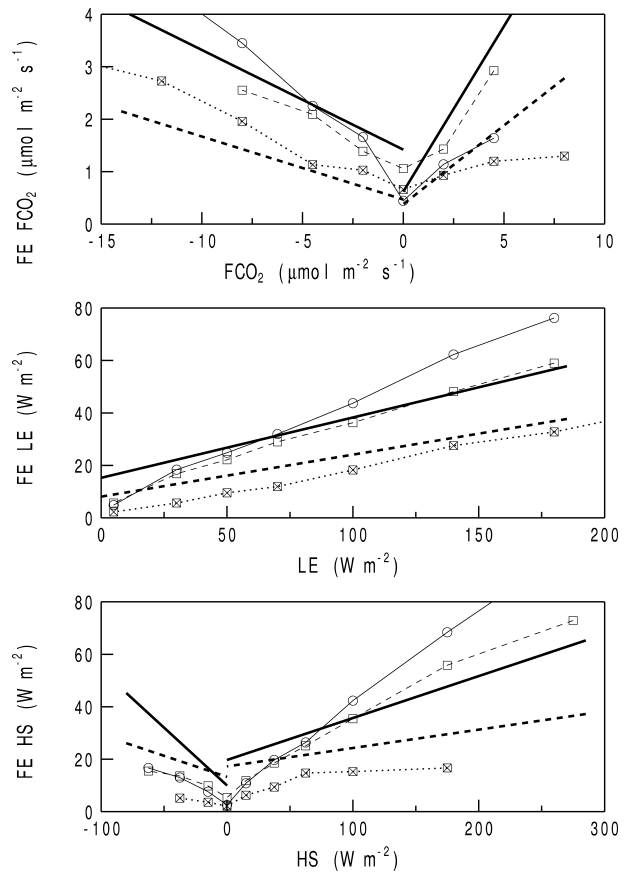nclude an important contribution from spatial heterogeneity, therefore enhancing the nocturnal flux uncertainty compared to more homogeneous sites. Footprint modelling (Appendix) shows that about 90% of the flux footprint is estimated to be within the young pine plantation during the day and more than 50% of the footprint is predicted to be outside the young site in the heterogeneous region at night, and the fraction of the footprint outside the site increases with increasing atmospheric stability. The footprint argument is consistent with the daytime results which show that when the flux footprint is in a homogeneous region at both pine forest sites, the average RFE values are approximately the same at both sites for all three scalars (Table 1).

Further evidence of the heterogeneity problem at the young pine forest is shown in Fig. 8 . Small values of the stability parameter, z/L, where L is the Obukov length scale, are associated with cloudy windy nights and a flux footprint closer to the tower in the homogeneous plantation, and large values of z/L are
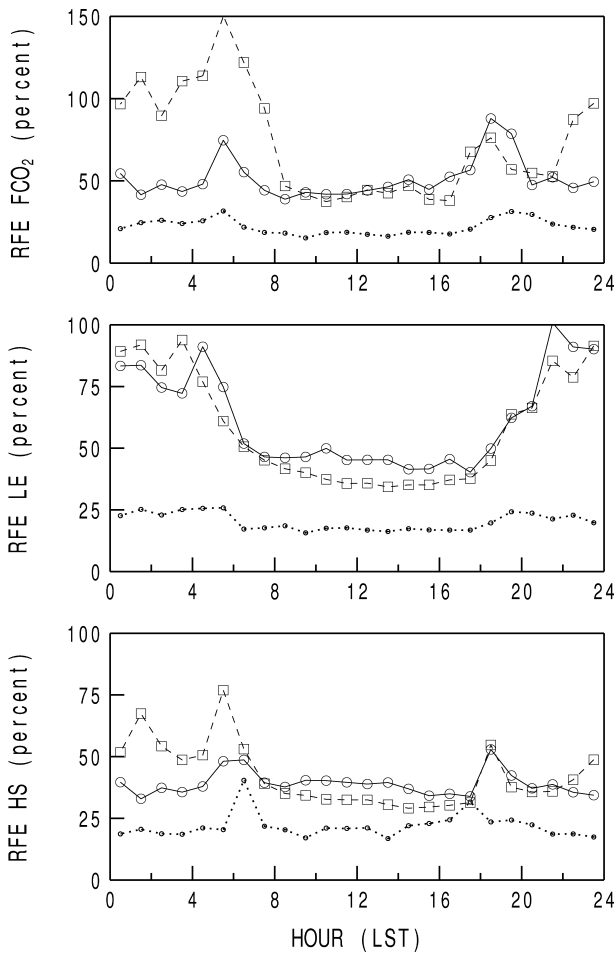
Fig. 6. Diurnal pattern of the relative flux uncertainty (RFE) during the strong growth season (May–June–July of 2004–2005 combined) for the mature pine (circles, solid) and young pine (squares, dash) forests, and for the maize data set (dots) in June–July of 2005.

Table 1. Relative flux uncertainty (RFE, eq. 3, percent) by time of day for the CO_2 flux (FCO_2), the latent heat flux (LE) and the sensible heat flux (HS) averaged over daytime (0900–1600) and nighttime (2200–0500) h for the mature pine (MP) and young pine (YP) forests during the strong growth season (May–June–July of 2004–2005 combined), and for the maize site in June–July 2005. Values in parenthesis are the between-hour standard deviation ($N = 7$ h)

	MP	YP	Maize
Day			
FCO_2	45 (3)	42 (3)	18 (1)
LE	45 (3)	36 (2)	17 (1)
HS	39 (2)	32 (2)	20 (2)
Night			
FCO_2	47 (4)	101 (11)	23 (2)
LE	84 (8)	86 (7)	23 (2)
HS	36 (2)	52 (8)	19 (1)

Table 2. Dimensional flux uncertainty (FE, eq. 2) of CO_2 (μmol m^{-2} s^{-1}), latent heat (W m^{-2}) and sensible heat (W m^{-2}) corresponding to the RFE estimates in Table 1

	MP	YP	Maize
Day			
FCO_2	3 (0.3)	2 (0.1)	5 (0.6)
LE	57 (6)	39 (3)	40 (5)
HS	93 (12)	61 (7)	14 (2)
Night			
FCO_2	0.9 (0.1)	2 (0.2)	1 (0.1)
LE	6 (0.7)	6 (1)	3 (0.6)
HS	10 (1)	12 (1)	4 (0.3)

associated with clear sky weak wind nights with strong stability and a footprint in the region with heterogeneous vegetation. Our interpretation is that the larger observed increase in the RFE for sensible heat with increasing stability at the young plantation, compared to the more homogeneous sites, is consistent with a more heterogeneous footprint in stronger stability at the young site. The nocturnal temperatures may be strongly influenced by heterogeneity in the vegetation due to radiative and mixing effects, where the surface radiational cooling is stronger in the clearings (Gustavsson et al., 1998). If the cold air that collects in the clearings were intermittently mixed out, that would introduce additional variability into the sensible heat flux.

If the subrecord and daily-differencing approaches were nearly equivalent methods for estimating flux uncertainty, then we might expect to find similar results for the mature and young pine forest sites compared to those reported by Richardson et al. (2006) for their forest composite. This is approximately the case

for the daytime fluxes, however, our nocturnal flux uncertainty estimates are generally smaller. In addition, we might expect similar uncertainty estimates for the maize site and their grassland site. This is generally the case for the daytime CO_2 and latent heat fluxes, but not for the daytime sensible heat flux or the nocturnal fluxes, where our uncertainty estimates are smaller. In summary, the subrecord approach used here leads to smaller flux uncertainty estimates compared to the daily-differencing approach at night.

Possible causes for larger estimates of flux uncertainty from the daily-differencing approach were described earlier (see Section 1). In addition, differences on weak wind nights may be partially due to the the choice of the perturbation timescale (Section 3). This effect is clearly evident at the maize site, where for nocturnal winds less than 1 m s^{-1} the sensible heat flux variability is 50% larger using a 30-min perturbation timescale compared to using a 5-min timescale to calculate the flux (Fig. 9). Use of the shorter perturbation timescale reduces the flux uncertainty by
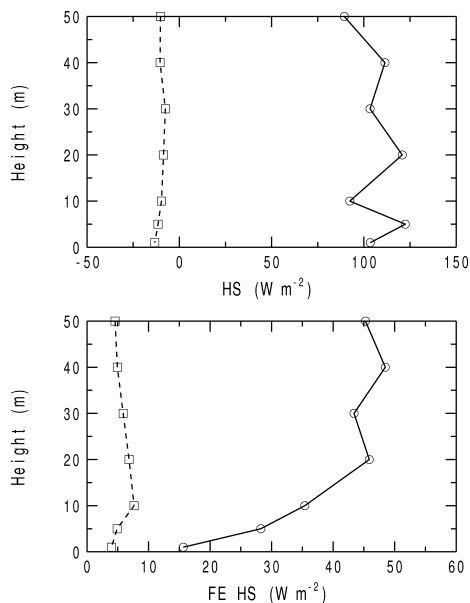
Fig. 7. Measurement height dependence (profile) of the flux and flux uncertainty for sensible heat in CASES (Kansas grassland) for unstable ($z/L < -0.25$, solid) and stable conditions ($z/L > 0.25$, dashed) in October of 1999. The corresponding unstable RFE values are 15, 23, 38, 38, 42, 44 and 50% for measurement heights of 1, 5, 10, 20, 30, 40 and 50 m above ground.
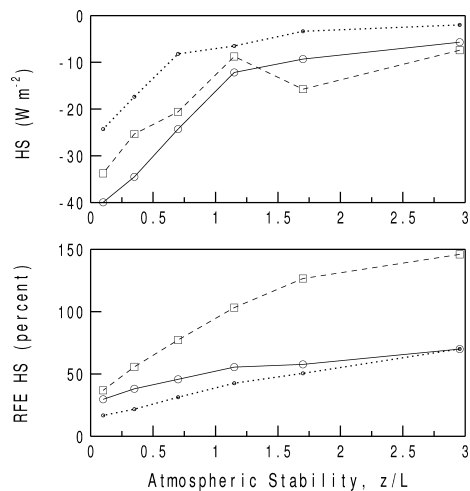

Fig. 8. Atmospheric stability dependence of the sensible heat flux and relative flux uncertainty (RFE) in the stable boundary layer during the strong growth season (May–June–July of 2004–2005 combined) for the mature pine (circles, solid) and young pine (squares, dash) forests, and for the maize data set (dots) in June–July of 2005.

filtering out the non-turbulent motions, which become relatively more important as the turbulence becomes weaker. The effect is also observed at the mature pine site and to a lessor degree at the young pine forest, although at the young site the stability dependence of the footprint (heterogeneity) is a complicating factor.
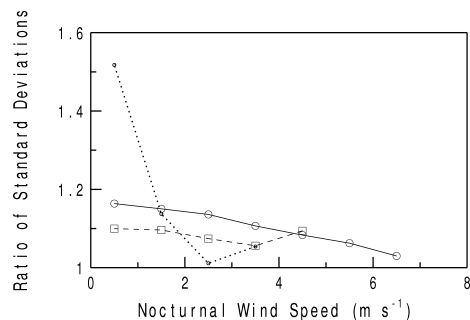

Fig. 9. The standard deviation of the sensible heat flux calculated using a 30-min perturbation timescale divided by the standard deviation using a 5-min perturbation timescale for different nocturnal wind speed categories during the strong growth season (May–June–July of 2004–2005 combined) for the mature pine (circles, solid) and the young pine (squares, dash) forests, and for the maize data set (dots) in June–July of 2005.

For daytime conditions, use of a shorter perturbation timescale (as in the subrecord method) might be expected to underestimate the flux uncertainty due to a failure to capture the largest (and therefore most poorly sampled) turbulence scales in convective conditions, however, this is not observed at the two forest sites (Fig. 5). The subrecord approach does yield smaller flux uncertainty estimates for sensible and latent heat at the maize site compared to the daily-differencing approach (and a 30-min perturbation timescale) applied to the grassland site.

4.2. Stability composites

Much of the previous discussion has been based on compositing the data by time of day for the growing season. The time of day analysis is useful because it represents the average diurnal cycle of the flux uncertainty, however it does not reflect the true stability dependence of the uncertainty. While there is a strong relationship between z/L and time of day on average, compositing by time of day understates the stability dependence. For example, moderate to strong winds result in small values of z/L regardless of the time of day or the strength of the surface heating or cooling. For these reasons, we expect that the unstable–stable difference in the RFE should be larger than the day-night difference. This is indeed the case (compare Figs. 6 and 10 , and Tables 1 and 3).

RFE increases with increasing stability for all scalars and all sites for $z/L >$ about 0.5 (Fig. 10). Only a weak stability-dependence is found for unstable to weakly stable conditions. This increase in uncertainty for the strongest stabilities may be related to the increased relative non-stationarity of the flow and the increased relative importance of heterogeneity in strongly stable conditions. Motions that are thought to contribute to non-stationarity (and therefore to the flux uncertainty) in the stable boundary layer include meandering of the wind (Hanna, 1983; Anfossi et al., 2005), internal gravity waves (Nappo, 2002),
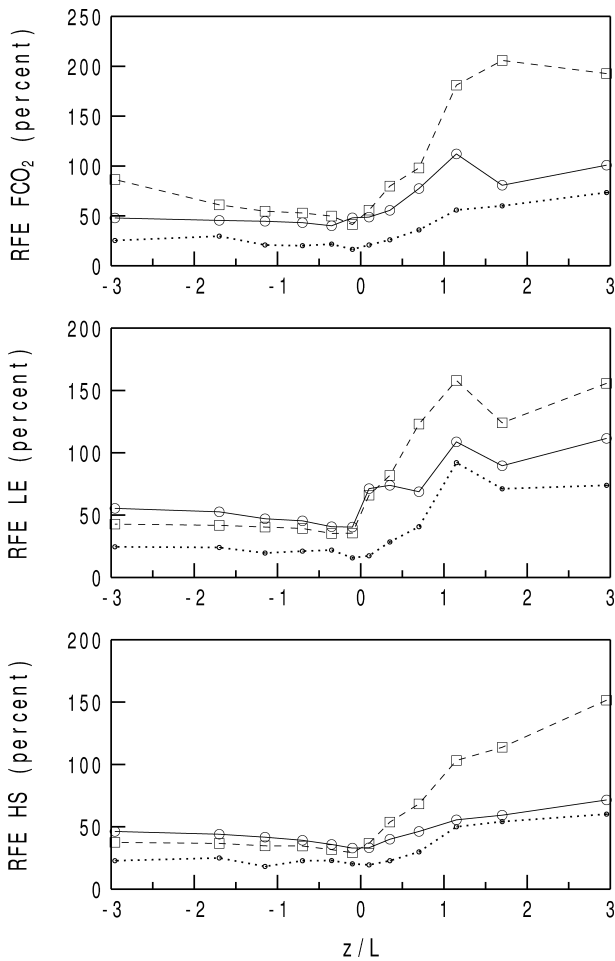
Fig. 10. Stability dependence of the relative flux uncertainty (RFE) during the strong growth season (May–June–July of 2004–2005 combined) for the mature pine (circles, solid) and young pine (squares, dash) forests, and for the maize data set (dots) in June–July of 2005.

Table 3. Relative flux uncertainty (RFE, eq. 3, percent) composited by atmospheric stability class instead of time of day

	MP	YP	Maize
$z/L < -1$			
FCO_2	46	67	25
LE	52	42	23
HS	44	37	22
$-1 < z/L < 1$			
FCO_2	52	63	24
LE	57	63	24
HS	38	42	23
$z/L > 1$			
FCO_2	98	193	63
LE	103	146	79
HS	62	123	55

density currents and solitary waves (Sun et al., 2004), pulsating drainage flows, vortical modes or fossil turbulence, wake vortices and numerous other modes (Mahrt et al., 2001, and references therein). Such motions can modulate the turbulence flux through modification of the wind shear, temperature stratification and scalar gradients.

The ratio of RFE for strongly stable conditions ($z/L > 1$) to RFE for strongly unstable conditions ($z/L < -1$) ranges from 1.4 (for sensible heat at mature pine) to 3.5 (latent heat at young pine) and averages 2.6 over all scalars and all sites. For all sites and all stability classes, the RFE for sensible heat is smaller than the RFE for latent heat or CO_2. This may be partially due to instrumental problems, where attack angle-dependent instrument separation is an issue for latent heat and CO_2, but not for sensible heat. The RFE estimates are smallest at the maize site for all scalars and all stability classes, probably due to the low measurement height and the homogeneous conditions, as discussed earlier. The largest RFE values in stable conditions at the young pine forest are probably associated with heterogeneity and large footprints in strong stability. While the RFE values are very large in strong stability, strongly stable conditions ($z/L > 1$ in Table 3 and Fig. 10) represent only 9, 4 and 5% of the total data at the mature pine, young pine and maize sites, respectively.

4.3. Classical sampling error

The observed RFE easily exceeds the theoretical prediction for the classical sampling error (RSE, eq. 4) for all scalars and all sites for day and night (Table 4). Even at the maize site, which could be considered close to ideal for flux measurements because of the long uniform fetch and flat terrain, the observed RFE is more than twice as large as the theoretical prediction of the random sampling error. This suggests that contributions to the flux uncertainty from sources other than classical sampling error are important during the day and night, even at sites considered to be homogeneous.

A possible source of daytime flux uncertainty due to instrumental problems may be time-dependent flow distortion

Table 4. Predictions for the classical random sampling error (RSE, eq. 4, percent) based on estimates of the flux integral timescale

	MP	YP	Maize
Day			
FCO_2	15	14	5
LE	18	14	5
HS	13	11	7
Night			
FCO_2	30	60	12
LE	55	79	14
HS	19	45	8

associated with the large attack angles of the flow in weak winds with strong convection (Nakai et al., 2006). Gash and Dolman (2003) found that a large fraction of the integrated daytime flux was carried by eddies with attack angles larger than the sonic anemometer manufacturer's suggested limit, even though the frequencies of occurrence of these large angles were relatively low. Another problem arises for daytime measurements made in the roughness sublayer (Raupach, 1992), where the flux varies with horizontal position because individual trees or small clumps of trees influence the flux. In the roughness sublayer small changes in wind direction (footprint) can contribute scatter to the flux. Katul et al. (1999) found significant spatial flux variability of 17% for sensible heat, 33% for latent heat and 27% for the CO_2 flux based on daytime flux measurements at seven towers separated by at least 100 m from each other over a uniform even-aged pine forest.

The largest RFE and RSE values are found for the young pine site at night. We have attributed the large nocturnal RFE at this site to modest heterogeneity in the flux footprint. The heterogeneity, and possibly disturbances associated with the change in aerodynamic roughness at the boundary of the young pine plantation, may increase the RSE estimate by decreasing the correlation between scalars and the vertical velocity. The smallest RSE estimates are found at the maize site during the day where strong correlation is found between fluctuations in scalars and vertical velocity.

5. Conclusions

A new observational approach for estimating turbulence flux uncertainty is applied to CO_2, latent heat and sensible heat flux data from two ponderosa pine forests in Oregon and a maize site in Iowa. The approach calculates the variability in the subrecord (5 min) fluxes to approximate the uncertainty in the record-averaged (1-h) flux. A summary of the results is given in Tables 1–4. Compared to other recently published methods of evaluating short-term flux uncertainty, the new method: (1) requires only a single flux tower and a single set of instruments (e.g. one sonic anemometer and one gas analyser), (2) can use all the available data, not just periods 24 hr apart with similar environmental conditions and (3) does not rely on interpretations of model minus observed flux residuals to represent uncertainty in the observations.

The dimensional flux uncertainty (FE) generally scales with the magnitude of the flux, in agreement with previous studies. The daytime composite relative flux uncertainty (RFE) varies by site more than by scalar, and is smaller at the maize site by a factor of two compared to the two forest sites. Averaging over the three scalars, the daytime RFE estimates are approximately 45% at the tall pine forest, 40% at the short pine plantation and 20% at the maize. The RFE increases with increasing measurement height, at least in the lowest 20 m above the ground in unstable conditions over a short grass canopy. Modest surface heterogeneity (a mix of tall trees, short trees and clearings) in the flux

footprint appears to approximately double the RFE compared to more homogeneous sites for all scalars. Footprint modeling suggests a stability-dependent heterogeneity at the pine plantation, where the footprint is in a more heterogeneous region at night compared to during the day, when the footprint is closer to the tower. The stronger heterogeneity at night may apply to other flux sites.

The new approach finds smaller RFE at night compared to previously published results using a daily-differencing approach. Smaller RFE for the new approach may be related to the 24-h differencing used in the daily-differencing method (see Section 1). For the weakest wind stable conditions, smaller uncertainty from the new method may be related to the 5-min perturbation timescale used to better capture turbulence and exclude longer timescale non-turbulent motions (Section 3). For the weakest wind nocturnal periods at the maize site, the RFE for sensible heat is 50% larger using a 30-min perturbation timescale to compute the flux compared to using the 5-min timescale. For these same periods, the turbulence flux is confined to timescales of a few minutes or less. The sensitivity of RFE to the choice of perturbation timescale decreases with increasing wind speed and turbulence intensity.

Compositing the RFE by time of day masks a strong stability dependence. While the time of day composites of RFE show little variation between day and night for the homogeneous sites, compositing by stability class (z/L) shows a strong increase in RFE with increasing stability for all scalars and all sites for z/L greater than about one-half. No clear stability dependence is found between unstable and weakly stable conditions. Contributions to the uncertainty from non-stationarity and heterogeneity are expected to be more important with the weaker horizontal and vertical mixing found in stable conditions.

The observed RFE estimates are larger then the theoretical predictions of the classical random sampling error for all scalars and all sites for day and night periods. This result suggests that contributions to the RFE from instrumental problems, non-stationarity and heterogeneity are important during the day and night even at sites considered homogeneous.

6. Acknowledgments

7. Appendix

The footprint analyses are performed with the Thomson (1987) forward Lagrangian stochastic trajectory model of Langevin

type (e.g. Wilson et al., 1983; Wilson and Sawford, 1996). The exact formulation of the footprint algorithms and the definition of the flow statistics above the roughness sublayer, including the effect of stability on the profiles, can be found in Rannik et al. (2003). The model can be applied to diabatic conditions, and also considers within-canopy flow effects. In addition to being carried downwind by horizontal advection, the particles are dispersed by turbulent diffusion in the vertical, alongwind and crosswind directions. As a forward approach relying on the inverted plume assumption (e.g. Schmid and Oke, 1988; Schmid, 2002), the model is restricted to horizontally homogeneous flow conditions. This restriction may lead to erroneous results in the presence of significant inhomogeneity, such as near the edge of a clearing. For further discussion on footprint models in complex terrain, please refer to Göckede et al. (2006).

To save computation time, the flux footprint estimates were pre-calculated for fixed combinations of stability, wind speed and turbulence intensity. Thirty-thousand particles were released for each meteorological scenario from a height equal to 0.01 times the canopy height. The particles were tracked until the upwind distance accounting for approximately 90% of the total flux was reached. The turbulence statistics required to run the model were taken from a conifer site with comparable canopy characteristics to the young pine site. These profiles were produced using the one-and-a-half order closure model by Massman and Weil (1999), based on measurements of leaf area index. Profiles in the roughness sublayer and the atmospheric boundary layer were fit to local measurements of the turbulence statistics (i.e. σ_u, σ_v and σ_w), vertical momentum flux and mean wind speed for representative cases of boundary layer stratification.

References

Acevedo, O. C., Moraes, O. L. L., Degrazia, G. A. and Medeiros, L. E. 2006. Intermittency and the exchange of scalars in the nocturnal surface layer. *Boundary-Layer Meteor.* **119**, 41–55.

Acevedo, O. C., Moraes, O. L. L., Fitzjarrald, D., Sakai, R. and Mahrt, L. 2007. Turbulent carbon exchange in very stable conditions. *Boundary-Layer Meteor.* **125**, 49–61.

Andreas, E. L., Hill, R. J., Gosz, J. R., Moore, D. I., Otto, W. D. and co-authors. 1998. Statistics of surface layer turbulence over terrain with meter-scale heterogeneity. *Boundary-Layer Meteor.* **86**, 378–408.

Anfossi, D., Oettl, D., Degrazia, G. and Goulart, A., 2005. Anemometer observations in low wind speed conditions. *Boundary-Layer Meteor.* **114**, 179–203.

Bendat, J. S. and Piersol, A. G. 1986. *Measurement and Analysis of Random Data.* John Wiley and Sons, New York, 330 pp.

Braswell, B. H., Sacks, W. J., Linder, E. and Schimel, D. S. 2005. Estimating diurnal to annual ecosystem parameters by synthesis of a carbon flux model with eddy covariance net ecosystem exchange observations. *Global Change Biol.* **11**, 335–355.

Caughey, S. J. and Readings, C. J. 1975. Turbulent fluctuations in convective conditions. *Q. J. R. Meteor. Soc.* **101**, 537–542.

Cosh, M. H., Kabela, E. D., Hornbuckle, B., Gleason, M. L., Jackson, T. J. and co-authors. 2009. Observations of dew amount using in situ

and satellite measurements in an agricultural landscape. *Agric. Forest Meteor.* **149**, 1082–1086.

Deardorff, J. W. and Willis, G. E. 1985. Further results from a laboratory model of the convective planetary boundary layer. *Boundary-Layer Meteor.* **32**, 205–236.

Dragoni, D., Schmid, H. P., Grimmond, C. S. B. and Loescher, H. W. 2007. Uncertainty of annual net ecosystem productivity estimated using eddy-covariance flux measurements. *J. Geophys. Res.* **112**, D17102, doi:10.1029/2006JD008149.

Feigenwinter, C., Bernhofer, C. and Vogt, R. 2004. The influence of advection on the short term CO_2 budget in and above a forest canopy. *Boundary-Layer Meteor.* **113**, 201–224.

Finkelstein, P. L. and Sims, P. F. 2001. Sampling error in eddy correlation flux measurements. *J. Geophys. Res.* **106**, 3503–3509.

Finnigan, J. 2004. Advection and modeling. In: *Handbook of Micrometeorology: A Guide for Surface Flux Measurement and Analysis* (eds X. Lee, W. Massman, B. Law). Kluwer Academic Publishers, Boston, 250.

Finnigan, J. J., Clement, R., Malhi, Y., Leuning, R. and Cleugh, H. A. 2003. A re-evaluation of long-term flux measurement techniques. Part I: averaging and coordinate rotation. *Boundary-Layer Meteor.* **107**, 1–48.

Foken, T., Göckede, M., Mauder, M., Mahrt, L., Amiro, B. and co-authors. 2004. Post-field data quality control. In: *Handbook of Micrometeorology: A Guide for Surface Flux Measurement and Analysis* (eds X. Lee, W. Massman, and B. Law). Kluwer Academic Publishers, Boston, 250.

Gash, J. H. C. and Dolman, A. J. 2003. Sonic anemometer cosine response and flux measurement. I. The potential for cosine error to affect sonic anemometer-based flux measurements. *Agric. Forest Meteor.* **119**, 195–207.

Göckede, M., Markkanen, T., Hasager, C. B. and Foken, T. 2006. Update of a footprint-based approach for the characterization of complex measurement sites. *Boundary-Layer Meteor.* **118**, 635–655.

Göckede, M., Foken, T., Aubinet, M., Aurela, M., Banza, J. and co-authors, 2008. Quality control of CarboEurope flux data. Part 1: coupling footprint analyses with flux data quality assessment to evaluate sites in forest ecosystems. *Biogeosciences* **5**, 433–450.

Gustavsson, T., Karlsson, M., Bogren, J. and Lindqvist, S. 1998. Development of temperature patterns during clear nights. *J. Appl. Meteor.* **37**, 559–571.

Hanna, S. R. 1983. Lateral turbulence intensity and plume meandering during stable conditions. *J. Appl. Meteor.* **20**, 242–249.

Hollinger, D. Y. and Richardson, A. D. 2005. Uncertainty in eddy covariance measurements and its application to physiological models. *Tree Physiol.* **25**, 873–885.

Howell, J. F. and Sun, J. 1999. Surface-layer fluxes in stable conditions. *Boundary-Layer Meteor.* **90**, 495–520.

Hunt, J. C. R. and Carlotti, P. 2001. Statistical structure at the wall of the high Reynolds number turbulent boundary layer. *Appl. Scient. Res.* **66**, 453–475.

Kaimal, J. C. and Finnigan, J. J. 1994. *Atmospheric boundary layer flows, their structure and measurements.* Oxford University Press, Oxford, 289 pp.

Katul, G., Hsieh, C., Bowling, D., Clark, K., Shurpali, N. and co-authors. 1999. Spatial variability of turbulent fluxes in the roughness sublayer of an even-aged pine forest. *Boundary-Layer Meteor.* **93**, 1–28.

Knorr, W. and Kattge, J. 2005. Inversion of terrestrial ecosystem model parameter values against eddy covariance measurements by Monte Carol sampling. *Global Change Biol.* **11**, 1–19.

Lasslop, G., Reichstein, M., Kattge, J. and Papale, D. 2008. Influences of observational errors in eddy flux data on inverse model parameter estimation. *Biogeosciences* **5**, 1311–1324.

Lee, Y.-H. and Mahrt, L. 2005. Effect of stability on mixing in open canopys. *Agric. Forest Meteor.* **135**, 169–179.

Lenschow, D. H., Mann, J. and Kristensen, L. 1994. How long is long enough when measuring fluxes and other turbulence statistics? *J. Atmos. Oceanic Technol.* **11**, 661–673.

Leuning, R., Zegelin, S. J., Jones, K., Keith, H. and Hughes, D. 2008. Measurement of horizontal and vertical advection of CO_2 within a forest canopy. *Agric. Forest Meteor.* **148**, 1777–1797.

Mahrt, L. 1998. Flux sampling errors for aircraft and towers. *J. Atmos. Oceanic Technol.* **15**, 416–429.

Mahrt, L. 2009. Characteristics of submeso winds in the stable boundary layer. *Boundary-Layer Meteor.* **130**, 1–14.

Mahrt, L. and Vickers, D. 2006. Extremely weak mixing in stable conditions. *Boundary-Layer Meteor.* **119**, 19–39.

Mahrt, L., Vickers, D. and Sun, J. 2001. Spatial variations of surface moisture flux from aircraft data. *Adv. Water Resour.* **24**, 1133–1141.

Mann, J. and Lenschow, D. H. 1994. Errors in airborne flux measurements. *J. Geophys. Res.* **99**, 14519–14526.

Massman, W. J. and Weil, J. C. 1999. An analytical one-dimensional second-order closure model of turbulence statistics and the Lagrangian time scale within and above plant canopys of arbitrary structure. *Boundary-Layer Meteor.* **91**, 81–107.

Nakai, T., van der Molen, M., Gash, J. H. C. and Kodama, Y. 2006. Correction of sonic anemometry angle of attack errors. *Agric. Forest Meteor.* **136**, 19–30.

Nappo, C. J. 2002. *An Introduction to Atmospheric Gravity Waves.* Academic Press, Amsterdam, The Netherlands, 297 pp.

Paw U. K. T., Baldocchi, D. D., Meyers, T. P. and Wilson, K. B. 2000. Correction of eddy-covariance measurements incorporating both advective effects and density fluxes. *Boundary-Layer Meteor.* **97**, 487–511.

Poulos, G. S., Blumen, B., Fritts, D., Lundquist, J., Sun, J. and co-authors. 2002. CASES-99: a comprehensive investigation of the stable nocturnal boundary layer. *Bull. Am. Meteor. Soc.* **83**, 555–581.

Rannik, Ü., Markkanen, T., Raittila, J., Hari, P. and Vesala, T. 2003. Turbulence statistics inside and over forest: influence on footprint prediction. *Boundary-Layer Meteor.* **109**, 163–189.

Raupach, M. R. 1992. Drag and drag partition on rough surfaces. *Boundary-Layer Meteor.* **60**, 375–395.

Raupach, M. R., Rayner, P. J., Barrett, D. J., Defries, R. S., Heimann, M. and co-authors. 2005. Model-data synthesis in terrestrial carbon observation: methods, data requirements and data uncertainty specifications. *Global Change Biol.* **11**, 378–397.

Richardson, A., Hollinger, D., Burba, G., Davis, K., Flanagan, L. and co-authors. 2006. A multi-site analysis of random error in tower-based measurements of carbon and energy fluxes. *Agric. Forest Meteor.* **136**, 1–18.

Richardson, A., Machecha, M., Falge, E., Kattge, J., Moffat, A. and co-authors. 2008. Statistical properties of random CO_2 flux measurement uncertainty inferred from model residuals. *Agric. Forest Meteor.* **148**, 38–50.

Schmid, H. P. 2002. Footprint modeling for vegetation atmosphere exchange studies: a review and perspective. *Agric. Forest Meteor.* **113**, 159–183.

Schmid, H. P. and Oke, T. R. 1988. Estimating the source area of a turbulent flux measurement over a patchy surface. *Proceedings of the 8th Symposium on Turbulence and Diffusion*, Boston, MA, American Meteorological Society, pp. 123–126.

Schwarz, P., Law, B. E., Williams, M., Irvine, J., Kurpius, M. and co-authors. 2004. Climatic versus biotic constraints on carbon and water fluxes in seasonally drought-affected ponderosa pine ecosystems. *Global Biochem. Cycle* **18**, GB4007,doi:10.1029/2004GB002234.

Sun, J., Lenschow, D., Burns, S., Banta, R., Newsom, R. and co-authors, 2004. Atmospheric disturbances that generate intermittent turbulence in nocturnal boundary layers. *Boundary-Layer Meteor.* **110**, 255–279.

Thomas, C. K., Law, B. E., Irvine, J., Martin, J. G., Pettijohn, J. C. and co-authors. 2009. Seasonal hydrology explains interannual and seasonal variation in carbon and water exchange in a semi-arid mature ponderosa pine forest in Central Oregon. *J. Geophys. Res.* **114**, G04006, doi:10.1029/2009JG001010.

Thomson, D. J. 1987. Criteria for the selection of stochastic models of particle trajectories in turbulent flows. *J. Fluid Mech.* **180**, 529–556.

Thorton, P. E., Law, B. E., Gholz, H. L., Clark, K. L., Falge, E. and co-authors. 2002. Modeling and measuring the effects of disturbance history and climate on carbon and water budgets in evergreen needle-leaf forests. *Agric. Forest Meteor.* **113**, 185–222.

van den Kroonenberg, A. and Bange, J. 2007. Turbulent flux calculation in the polar stable boundary layer: multiresolution flux decomposition and wavelet analysis. *J. Geophys. Res.* **112**, D06112, doi:10.1029/2006JD007819.

van Gorsel, E., Leuning, R., Cleugh, H., Keith, H. and Suni, T. 2007. Nocturnal carbon efflux: reconciliation of eddy covariance and chamber measurements using an alternative to the u_*-threshold filtering technique. *Tellus* **59B**, 397–403.

Vickers, D. and Mahrt, L. 1997. Quality control and flux sampling problems for tower and aircraft data. *J. Atmos. Oceanic Technol.* **14**, 512–526.

Vickers, D. and Mahrt, L. 2006a. A solution for flux contamination by mesoscale motions with very weak turbulence. *Boundary-Layer Meteor.* **118**, 431–447.

Vickers, D. and Mahrt, L. 2006b. Contrasting mean vertical motion from tilt correction methods and mass continuity. *Agric. Forest Meteor.* **138**, 93–103.

Vickers, D., Thomas, C. and Law, B. 2009. Random and systematic CO_2 flux sampling errors for tower measurements over forests in the convective boundary layer. *Agric. Forest Meteor.* **149**, 73–83.

Wilczak, J. M., Oncley, S. P. and Stage, S. A. 2001. Sonic anemometer tilt correction algorithms. *Boundary-Layer Meteor.* **99**, 127–150.

Williams, M., Schwarz, P., Law, B. E., Irvine, J. and Kurpius, M. 2005. An improved analysis of forest carbon dynamics using data assimilation. *Global Change Biol.* **11**, 89–105.

Wilson, J. D., Legg, B. J. and Thomson, D. J. 1983. Calculation of particle trajectories in the presence of a gradient in turbulent-velocity variance. *Boundary-Layer Meteor.* **27**, 163–169.

Wilson, J. D. and Sawford, B. L. 1996. Review of Lagrangian stochastic models for trajectories in the turbulent atmosphere. *Boundary-Layer Meteor.* **78**, 191–210.

Yilmaz, M. T., Hunt, E. R. and Jackson, T. J. 2008. Remote sensing of vegetation water content from equivalent water thickness using satellite imagery. *Remote Sens. Environ.* **112**, 2514–2522.